

Functional localization of single active ion channels on the surface of a living cell

Yuri E. Korchev*#, Yuri A. Negulyaev†, Christopher R.W. Edwards*, Igor Vodyanoy‡§ and Max J. Lab§

*Division of Medicine, Imperial College School of Medicine, MRC Clinical Sciences Centre, Hammersmith Campus, Du Cane Road, London W12 0NN, UK

†Institute of Cytology, Russian Academy of Sciences, Tichoretsky 4, St Petersburg, Russia

‡Office of Naval Research International Field Office, 223 Old Marylebone Road, London NW1 5TH, UK

§National Heart and Lung Institute, Imperial College School of Medicine, Charing Cross Campus, St Dunstan's Road, London W6 8RP, UK

#e-mail: y.korchev@ic.ac.uk

The spatial distribution of ion channels in the cell plasma membrane has an important role in governing regional specialization, providing a precise and localized control over cell function. We report here a novel technique based on scanning ion conductance microscopy that allows, for the first time, mapping of single active ion channels in intact cell plasma membranes. We have mapped the distribution of ATP-regulated K⁺ channels (K_{ATP} channels) in cardiac myocytes. The channels are organized in small groups and anchored in the Z-grooves of the sarcolemma. The distinct pattern of distribution of these channels may have important functional implications.

Regional specialization within a cell often requires a unique spatial distribution of individual membrane components such as ion channels and receptors to enable a precise, localized control over cell function. A good example is the neuromuscular junction where the location and density of ion channels/ionotropic membrane receptors are responsible for synaptic transmission. Nerve impulses induce Na⁺ channels in the target muscle cell to redistribute, immobilize and co-localize with acetylcholine receptors at sites of neuronal contact¹. In contrast, at extrajunctional regions the Na⁺ channel density is lower, and the channels are mobile². Another example is Na⁺-reabsorbing epithelia where amiloride-sensitive Na⁺ channels facilitate sodium transport and are restricted to the apical cell membrane³. These channels may also be non-uniformly distributed in the apical plasma membrane, and microvilli protruding from the cell bodies may carry more sodium channels than other parts of the membrane⁴. Non-random distributions have been also suggested for other types of ion channel^{5–11}.

Two major methodological approaches have been used to study the distribution of ion channels in the cell membrane. One uses specific markers for the ion channel proteins which can be visualized by microscopy-based techniques (for example, electron^{5,6}, optical^{5,12,13} or scanning probe microscopy⁴). Specific labelling is commonly achieved by immunostaining^{3,5,13} or with toxins⁸. The difficulties of identifying specific markers, low ion channel density, and non-specific staining of the sample limit the applicability of these methods, however. Moreover, staining can alter ion-channel function, and sample preparation often requires cell fixation. The green fluorescent protein (GFP) technique¹² may preserve the functional integrity of ion channel proteins. However, this method does not permit visualization of the native ion channels; only the additionally expressed, 'alien' ion channel proteins, hyperexpression of which may also alter cell function.

The second approach uses either patch-clamp^{14,15} or loose patch-clamp^{1,16,17} techniques to measure the local ion current across the plasma membrane, or fluorescent microscopy methods¹⁸ to monitor regional ion dynamics. This allows the activity of ion channels to be monitored in localized regions of the intact cellular

membrane. There are two methods that record the induced whole-cell current in conjunction with the localized activation of ion channels by the liberation of 'caged' mediators with two-photon absorption-mediated photoactivation⁹ or by local extracellular stimulation through a loose-seal pipette¹⁹. None of these methods is, however, capable of localizing individual functional ion channels in intact cellular membranes.

Here we describe a new method that allows, for the first time, mapping of single active ion channels with simultaneous high-resolution imaging of intact cellular membranes.

Results

Microscopy system for functional localization of ion channels. In essence, the system combines the peerless capability of the patch-clamp technique²⁰ to investigate the functions of single ion channels and another unique but relatively novel technique—scanning probe microscopy (SPM). The latter uses a glass micropipette as a scanning probe^{21–25} and allows high-resolution imaging and micromanipulation of the sample. The SPM part of the instrument is a scanning ion conductance microscope (SICM)^{21,23,25} that consists of the micropipette probe and a computer-controlled three-axis translation stage with measurement and feedback systems. The x and y axes of the translation stage are driven so as to scan the micropipette probe over the specimen, while recording the ion current through the probe tip. The position of the tip relative to the sample surface strongly influences the ion current through the pipette, which provides the feedback signal to control the vertical position of the tip. This ensures that the sample and probe do not come into contact with one another. The use of a micropipette as a SPM probe provides two distinct advantages in cell imaging and mapping of ion channels in intact cell membranes. First, it provides a non-invasive scanning protocol that prevents the tip of the micropipette making direct physical contact with the specimen by maintaining a constant distance between the probe and the sample²³. Second, it enables the direct stimulation of single ion channels on the cell surface. This is achieved by the highly localized application of ions, agonists or other agents to the membrane during the

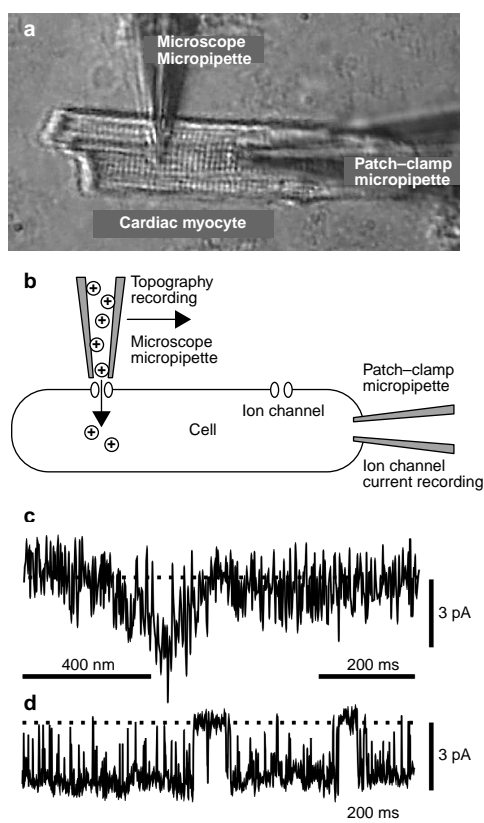


Figure 1 Functional localization of single ion channels in intact cell membranes. **a**, Photograph of the experimental arrangement with two micropipettes. **b**, Diagram of the sensing mechanism of the combined SICM/whole-cell voltage-clamp technique. **c**, Detection of a single K_{ATP} channel position in rat cardiomyocyte sarcolemma. A single-channel current record obtained during a single profile scan over the cell surface. **d**, A single K_{ATP} channel current record observed in an outside-out patch under ionic conditions similar to those in **c** (see Methods), where the bath K^+ concentration was equal to that supplied by the scanning micropipette.

scan via the microscope micropipette, while monitoring the electrical response of the cell with the patch-clamp micropipette (Fig. 1). **Localization of ATP-regulated K^+ channels in cardiac myocytes.** We have applied this method to investigate the distribution of ATP-regulated K^+ channels^{26,27}, which have important roles in the relaxation and preservation of cardiomyocytes during metabolic stresses²⁷ such as hypoxia or ischaemia. Very little is known about their localization in the cell membrane. The experimental conditions were designed so that intra- and extracellular solutions contained no K^+ ions, and the intracellular ATP concentration was reduced to provide maximum activation of K_{ATP} channels. Under these conditions, when a microscope micropipette filled with K^+ ions scans the surface of a cardiac myocyte and passes over the active channel, the patch-clamp micropipette records increased K^+ current (Fig. 1c). The observed ion-current profile is bell shaped, which is as expected from the distribution of K^+ ions around the micropipette tip. The maximum value of negative current corresponds to the position of the scanning micropipette tip when it is exactly above the ion channel, and is proportional to the K^+ concentration in the micropipette. This value closely matches the amplitude of single K_{ATP} channel currents observed in outside-out patches studied under similar ionic conditions (Fig. 1d), where the bath K^+ concentration is equal to that supplied by the scanning micropipette.

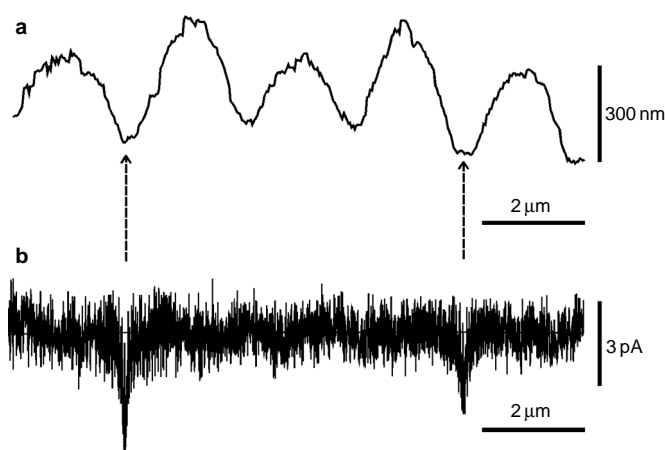


Figure 2 Simultaneous topographic and ion-channel current recording. **a**, A single topographic profile of cardiac myocyte sarcolemma. **b**, A matching K^+ current record. The arrows indicate the positions of single K_{ATP} channels on the cell surface.

These procedures allow us to obtain two images simultaneously (shown as the single profiles across a cardiac myocyte surface in Fig. 2a, b). One is the topographical image of the cell surface (Fig. 2a). The other is an 'ion current' image (Fig. 2b), where each point corresponds to the value of ion current measured by the patch-clamp pipette. This is plotted using the coordinates of the microscope micropipette tip on the cell surface at the time of measurement. There are two clearly visible, downward-directed current peaks in Fig. 2b. These correspond to the individual K_{ATP} channels where vertical arrows indicate their positions on the cardiac myocyte surface (Fig. 2a).

The opening of large-conductance ion channels just beneath the probe tip might interfere with SICM scanning, forcing a control system to readjust the tip position towards the sample. This could produce unwanted topographical artefacts. We estimated that in our experiments the inaccuracy of height measurement attributed to the potassium current was less than 0.1 nm, which is much less than the present SICM resolution (~50 nm).

Active ion channels spend part of the time in the closed state and can easily remain undetected during a short period of measurement. To increase the probability of detecting single channels, we acquired the current through the same single channel during several profile records of the scan similar to one shown in Fig. 1c. For example, the left of the three single channels visualized in Fig. 3a shows a relatively smaller current peak. However, the single profile records (not shown for this channel) indicate that it has the same open-state current amplitude as the other channels but happens to spend more time in the closed state during the time of observation. The open probability for this channel was estimated to be 0.18 compared with 0.6 and 0.8 for the other two. These results raise the possibility that for the first time one can acquire the position and the functional characteristics of individual ion channels in intact cellular membranes. Analysis of a large number of current images reveals that K_{ATP} channels are non-uniformly distributed, being concentrated in the localized regions of the cardiac myocyte sarcolemma (for example, Fig. 3c). Each of these regions or 'clusters' is separated by 2–6 μm from the others and contains up to 10 active ion channels. The ion channels within the 'cluster' are 0.2–1 μm apart.

We have also found that the K_{ATP} channels can be recorded at the same locations in the sarcolemma during relatively long periods of observation (more than 40 min). This suggests that these channels have low lateral mobility. Furthermore, the active K_{ATP} channels are

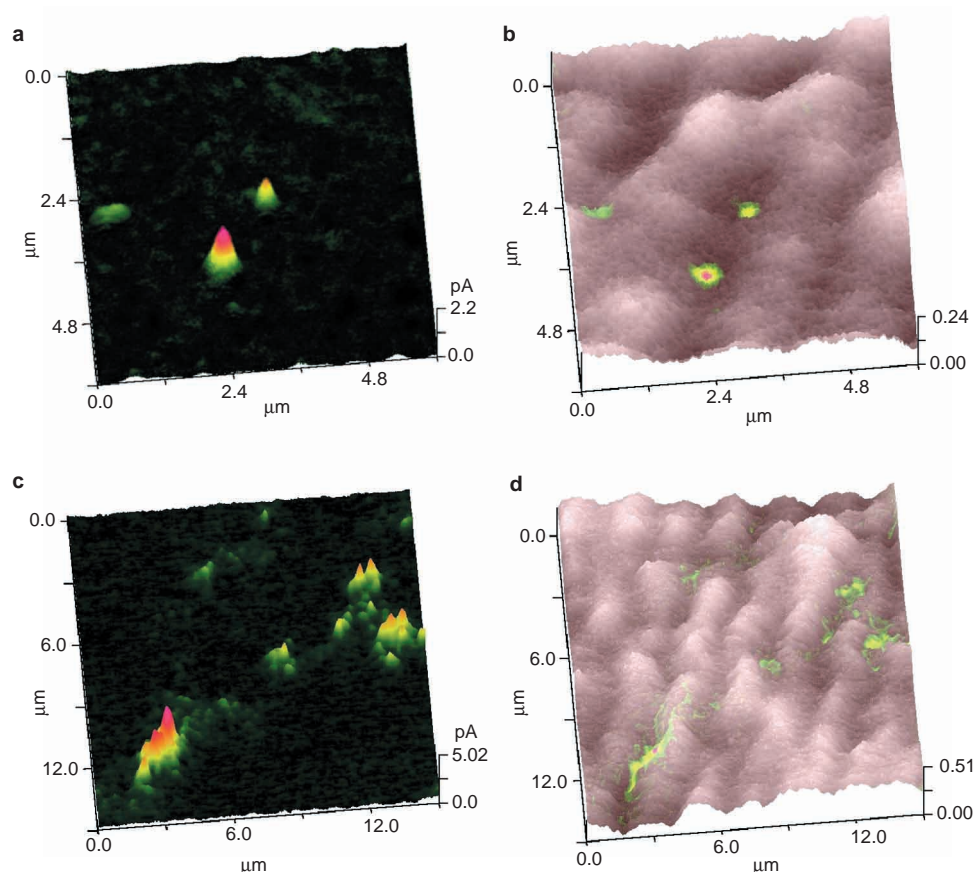


Figure 3 Functional imaging of the distribution of single K_{ATP} channels in the cardiomyocyte sarcolemma. **a–d**, Maps of K^+ current (**a**, **c**) and of surface topography superimposed on the K^+ current map (**b**, **d**) of a small area of a single, quiescent cardiac myocyte. Individual K_{ATP} channels are detected in the parallel

grooves (Z-grooves) of the cardiac myocyte sarcolemma; their visibility is partially obscured by the three-dimensional scalloped features of the cell surface (**b**, **d**). Imaging was performed so that each scanning raster increment step is at least one-tenth of the diameter of the microscope micropipette tip.

observed only in ‘scallop’-like regions of sarcolemma (for example, Fig. 3), and not in other parts of the plasma membrane (for example, the regions of cellular contacts). We estimated the channel density in these scalloped regions of sarcolemma to be 5–10 K_{ATP} channels per $100 \mu m^2$, which is slightly higher than average channel density in the whole cardiac myocyte sarcolemma (2–5 K_{ATP} channels per $100 \mu m^2$) estimated from whole-cell current data. This is expected from the averaging of high and low channel density regions. Superimposing the K^+ current distribution on the sarcolemma surface topography reveals that the K_{ATP} channels align along the grooves that are over the I bands of the main contractile elements (Fig. 3b, d). These are the regions where the plasmalemma is anchored to an intracellular cytoskeleton to form Z-grooves and so give cardiac myocytes a characteristic scalloped surface.

Discussion

Our results show that the K_{ATP} channels hold their position on the cell surface for a relatively long time. This suggests that the channels are most likely anchored by the cytoskeleton in the sarcolemma. Published results also indicate that there is a link between the F-actin cytoskeleton and the K_{ATP} channels²⁸. Moreover, the channel positions are found in the Z-grooves—the sarcolemma regions that strongly interact with the intracellular cytoskeleton. It is from these grooves that the transverse tubules (T-tubules) emanate; one of their functions is presumed to be propagation of the action potential²⁹. The fact that the K_{ATP} channels are involved in controlling

propagation of the action potential³⁰, together with our observed clustering of K_{ATP} channels close to the T-tubule openings suggests that this proximity could provide a precise, localized, as yet unrecognized control over propagation of the action potential along the T-tubule system. This could be especially important during metabolic changes in cardiac myocytes (hypoxia, ischaemia) when a significant drop in ATP concentration can trigger K_{ATP} channel opening, resulting in the action potential shortening³⁰.

The technique described in this paper is designed for imaging the distribution of ion-specific channels. The technique could also be adapted to map the localization of ligand-regulated, mechanosensitive or voltage-gated ion channels, as the microscope micropipette probe can be used to deliver defined chemical, electrical or mechanical stimuli to the localized regions of the cell surface during the scan. Also, the technique will have general applications in the investigation of ion channel functional localization in intact cell membranes of different cell types.

Methods

Patch-clamp recording.

Standard patch-clamp techniques operating in the whole-cell and outside-out modes were used as described previously²⁰. The patch-clamp micropipettes were made from 1 mm outer diameter, 0.58 mm inner diameter glass microcapillaries (Intracel) using a laser-based Brown-Flaming puller (model P-2000, Sutter Instrument Company). Before use, the micropipettes were fire polished to produce tip diameters of $\sim 2 \mu m$. The pipette was gently sucked on to the myocyte at a point fairly remote from the area intended for topographical scanning. The ion channel currents were measured with an Axopatch 200B patch-clamp amplifier (Axon Instruments). Current signals were low-pass filtered at 200 Hz,

digitized and analysed with continuous data acquisition hardware and software (Axon DigiPack 1200, Axon Instruments).

Scanning ion conductance microscopy.

The basic arrangement of the SCIM for topographical imaging of living cells was described previously^{23,24}. The microscope micropipettes were made from the same glass microcapillaries as the patch-clamp micropipettes. We estimated the tip radius of the microscope micropipettes used in the present series of experiments to be ~100 nm, and the cone angle of the tip to be ~1.5°. The set-point current for the SCIM feedback control was ~3 nA.

Combined whole-cell voltage clamp and SCIM imaging system.

The microscope micropipette provides local application of ions to the cell surface/ion channel during the scan while the patch-clamp micropipette records the cellular electrical response (Fig. 1a, b). High current sensitivity and low noise recording was achieved by adjusting the experimental conditions such that the intracellular and extracellular solutions were replaced with solutions containing ions that do not permeate through the ion channel of interest. The microscope micropipette contained permeable ions and as it scanned the cell surface it supplied these ions to a highly localized region (of the order of the tip size, 50–200 nm). When the microscope tip passed over active ion channel(s) it created a strong electrochemical gradient for the permeable ions across the ion channel and the patch-clamp micropipette then immediately recorded an increase in ion-channel current.

For detection of single K_{ATP} channel positions in the rat cardiomyocyte sarcolemma, the cell was clamped in the whole-cell configuration with a patch-clamp micropipette containing K^+ and ATP-free solution (in mmol l⁻¹): 140 CsCl, 2.2 CaCl₂, 1.2 MgCl₂, 2.2 EGTA, and 10 HEPES/TrisOH pH 7.3. The extracellular solution also had no potassium ions. Under these conditions and at 0 mV membrane potential, the patch-clamp micropipette recorded nearly zero whole-cell current. This provided the necessary conditions for detection of single K^+ channels in the whole-cell configuration.

Before channel mapping, extracellular Na^+ was replaced for a short time by K^+ to ensure that the intracellular ATP level was sufficiently low to observe strong ATP-regulated K^+ current. Under these conditions, but in the presence of ATP in the patch-clamp micropipette, this current was not observed. The micropipette probe contained K^+ ions and as it was scanned over the cell surface it supplied K^+ to a highly localized area under the micropipette tip (Fig. 1b). Slight positive pressure (20 mm Hg above atmospheric pressure) was kept in the microscope micropipette to maintain a constant K^+ concentration under the tip, even during a relatively rapid scan (25 μ m s⁻¹). The higher ionic strength micropipette solution (in mmol l⁻¹: 145 KCl, 855 potassium aspartate, 2.0 CaCl₂, 1.0 MgCl₂, and 10 HEPES/TrisOH pH 7.3) was used to increase the probe current. This current was monitored to ensure that the application of potassium ions was not interrupted during the scan.

The K^+ distribution under the probe is determined by the diffusion of potassium ions out of the micropipette tip, yielding the highest K^+ concentration just beneath the probe, which is rapidly diluted outside the probe tip by the bath solution. The dimension of this region with the effective ion concentration could be defined with an 'diffusion radius', which in the present series of experiments we estimated was ~200 nm. During the scan, when the K^+ concentration increased near the active ion channel (within the 'diffusion radius' distance) the patch-clamp micropipette recorded increased K^+ current (Figs 1c and 2b). During raster scanning, this current was recorded, simultaneously with cell topography, using the coordinates of the microscope micropipette tip on the cell surface. This produced an 'ion current' image, where current peaks correspond to the positions of single ion channels on the cell surface (for example, Figs 2 and 3). The ion-channel current peaks had the expected bell shape (see Fig. 1c) and the full width at half maximum matched the estimated 'diffusion radius'. Superimposition of the K^+ current distribution on the cell-surface topography provided the exact positions of K_{ATP} channels on the cardiac myocyte sarcolemma (see Fig. 3c, d).

Cardiac myocytes.

Quiescent rat cardiac myocytes were isolated by digestion of intact perfused ventricle as previously described³¹. Cells were imaged on a glass coverslip at room temperature in K^+ -free solution containing (in mmol l⁻¹): 145 NaCl, 2.0 CaCl₂, 1.0 MgCl₂, and 10 HEPES/TrisOH pH 7.3.

RECEIVED 19 APRIL 2000; REVISED 8 MAY 2000; ACCEPTED 30 MAY 2000;
PUBLISHED 16 AUGUST 2000.

1. Beam, K. G., Caldwell, J. H. & Campbell, D. T. Na channels in skeletal muscle concentrated near the neuromuscular junction. *Nature* **313**, 588–590 (1985).
2. Angelides, K. J. Fluorescently labelled Na^+ channels are localized and immobilized to synapses of innervated muscle fibres. *Nature* **321**, 63–66 (1986).
3. Tousson, A., Alley, C. D., Sorscher, E. J., Brinkley, B. R. & Benos, D. J. Immunohistochemical localization of amiloride-sensitive sodium channels in sodium-transporting epithelia. *J. Cell Sci.* **93**, 349–362 (1989).
4. Smith, P. R., Bradford, A. L., Schneider, S., Benos, D. J. & Geibel, J. P. Localization of amiloride-sensitive sodium channels in A6 cells by atomic force microscopy. *Am. J. Physiol.* **272**, C1295–C1298 (1997).

5. Abrami, L. *et al.* Localization of the FA-CHIP water channel in frog urinary bladder [published erratum appears in *Eur. J. Cell Biol.* 1998 Jan;75(1):77]. *Eur. J. Cell Biol.* **73**, 215–221 (1997).
6. Alonso, G. & Widmer, H. Clustering of KV4.2 potassium channels in postsynaptic membrane of rat supraoptic neurons: an ultrastructural study. *Neuroscience* **77**, 617–621 (1997).
7. Barbosa, C. T., Alkondon, M., Aracava, Y., Maelicke, A. & Albuquerque, E. X. Ligand-gated ion channels in acutely dissociated rat hippocampal neurons with long dendrites. *Neurosci. Lett.* **210**, 177–180 (1996).
8. Cohen, M. W., Jones, O. T. & Angelides, K. J. Distribution of Ca^{2+} channels on frog motor nerve terminals revealed by fluorescent omega-conotoxin. *J. Neurosci.* **11**, 1032–1039 (1991).
9. Denk, W. Two-photon scanning photochemical microscopy: mapping ligand-gated ion channel distributions. *Proc. Natl Acad. Sci. USA* **91**, 6629–6633 (1994).
10. Frosch, M. P. & Dichter, M. A. Non-uniform distribution of GABA activated chloride channels in cultured cortical neurons. *Neurosci. Lett.* **138**, 59–62 (1992).
11. Karpen, J. W., Loney, D. A. & Baylor, D. A. Cyclic GMP-activated channels of salamander retinal rods: spatial distribution and variation of responsiveness. *J. Physiol. (Lond)* **448**, 257–274 (1992).
12. Grabner, M., Dirksen, R. T. & Beam, K. G. Tagging with green fluorescent protein reveals a distinct subcellular distribution of L-type and non-L-type Ca^{2+} channels expressed in dysgenic myotubes. *Proc. Natl Acad. Sci. USA* **95**, 1903–1908 (1998).
13. Joe, E. H. & Angelides, K. Clustering of voltage-dependent sodium channels on axons depends on Schwann cell contact. *Nature* **356**, 333–335 (1992).
14. Marrion, N. V. & Tavalin, S. J. Selective activation of Ca^{2+} -activated K^+ channels by co-localized Ca^{2+} channels in hippocampal neurons. *Nature* **395**, 900–905 (1998).
15. Almers, W., Stanfield, P. R. & Stühmer, W. Lateral distribution of sodium and potassium channels in frog skeletal muscle: measurements with a patch-clamp technique. *J. Physiol. (Lond)* **336**, 261–284 (1983).
16. Shrager, P. The distribution of sodium and potassium channels in single demyelinated axons of the frog. *J. Physiol. (Lond)* **392**, 587–602 (1987).
17. Ruff, R. L. Sodium channel slow inactivation and the distribution of sodium channels on skeletal muscle fibres enable the performance properties of different skeletal muscle fibre types. *Acta Physiol. Scand.* **156**, 159–168 (1996).
18. Stockbridge, N. & Ross, W. N. Localized Ca^{2+} and calcium-activated potassium conductances in terminals of a barnacle photoreceptor. *Nature* **309**, 266–268 (1984).
19. Anson, B. D. & Roberts, W. M. A novel voltage clamp technique for mapping ionic currents from cultured skeletal myotubes. *Biophys. J.* **74**, 2963–2972 (1998).
20. Hamill, O. P., Marty, A., Neher, E., Sakmann, B. & Sigworth, F. J. Improved patch-clamp technique for high-resolution current recording from cells and cell-free membrane patches. *Pflügers Arch.* **391**, 85–100 (1981).
21. Hansma, P. K., Drake, B., Marti, O., Gould, S. A. & Prater, C. B. The scanning ion-conductance microscope. *Science* **243**, 641–643 (1989).
22. Bard, A. J. *et al.* Chemical imaging of surfaces with the scanning electrochemical microscope. *Science* **254**, 68–74 (1991).
23. Korchev, Y. E. *et al.* Specialized scanning ion-conductance microscope for imaging of living cells. *J. Microsc.* **188**, 17–23 (1997).
24. Korchev, Y. E., Bashford, C. L., Milovanovic, M., Vodyanov, I. & Lab, M. J. Scanning ion conductance microscopy of living cells. *Biophys. J.* **73**, 653–658 (1997).
25. Korchev, Y. E. *et al.* Cell volume measurement using scanning ion conductance microscopy. *Biophys. J.* **78**, 451–457 (2000).
26. Noma, A. ATP-regulated K^+ channels in cardiac muscle. *Nature* **305**, 147–148 (1983).
27. Nichols, C. G. & Lederer, W. J. Adenosine triphosphate-sensitive potassium channels in the cardiovascular system. *Am. J. Physiol.* **261**, H1675–H1686 (1991).
28. Yokoshiki, H., Katsube, Y., Sunugawa, M., Seki, T. & Sperelakis, N. Disruption of actin cytoskeleton attenuates sulfonylurea inhibition of cardiac ATP-sensitive K^+ channels. *Pflügers Arch.* **434**, 203–205 (1997).
29. Cheng, H., Cannell, M. B. & Lederer, W. J. Propagation of excitation-contraction coupling into ventricular myocytes. *Pflügers Arch.* **428**, 415–417 (1994).
30. Lederer, W. J., Nichols, C. G. & Smith, G. L. The mechanism of early contractile failure of isolated rat ventricular myocytes subjected to complete metabolic inhibition. *J. Physiol. (Lond)* **413**, 329–349 (1989).
31. Harding, S. E. *et al.* Contractile responses of isolated rat and rabbit myocytes to isoproterenol and calcium. *J. Mol. Cell. Cardiol.* **20**, 635–647 (1988).

ACKNOWLEDGEMENTS

We thank S. Harding (National Heart and Lung Institute, Imperial College) for providing cardiac cells. Our work is supported by the Paul Instrument Fund, the British Heart Foundation, the Office of Naval Research and the Russian Foundation for Basic Research. Correspondence and requests for materials should be addressed to Y.E.K.